Surface Science 229 (1990) 290–297
North-Holland

TRANSPORT THROUGH ZERO-DIMENSIONAL STATES IN A QUANTUM DOT

Leo P. KOUWENHOVEN, Bart J. van WEES, Kees J.P.M. HARMANS
Faculty of Applied Physics, Delft University of Technology, P.O. Box 5046, 2600 GA Delft, The Netherlands

and

John G. WILLIAMSON
Philips Research Laboratories, 5600 JA Eindhoven, The Netherlands

Received 11 July 1989; accepted for publication 14 September 1989

We have studied the electron transport through zero-dimensional (0D) states. 0D states are formed when one-dimensional edge channels are confined in a quantum dot. The quantum dot is defined in a two-dimensional electron gas with a split gate technique. To allow electronic transport, connection to the dot is arranged via two quantum point contacts, which have adjustable selective transmission properties for edge channels. The 0D states show up as pronounced oscillations in the conductance (up to 40% of e^2/h), when the flux enclosed by the confined edge channel is varied, either by changing the magnetic field or the gate voltage. A prerequisite for the appearance of 0D states is that the transport through the entire device is adiabatic (i.e. with conservation of quantum numbers), which will be shown to occur at high magnetic field. The experimental results are in good agreement with theory and show that in the ballistic quantum Hall regime the current is carried entirely by edge channels.

1. Introduction

Advancing technology has made it possible to study the transport properties of a two-dimensional electron gas (2DEG) in the ballistic regime, for which the device dimensions must be much smaller than the elastic mean free path. One of the results is the observation of the quantum Hall effect (QHE) in ballistic submicron structures [1]. This observation shows that localized states cannot be a prerequisite for the appearance of quantized Hall plateaus. An alternative approach to explain the QHE is based on the formation of edge channels when a high magnetic field is applied perpendicular to the 2DEG [2]. The description of the QHE can then be given within the Landauer–Büttiker formalism for electron transport [3]. Besides their importance for explaining the QHE, edge channels have some fundamental properties which are interesting for further study. The electron transport in edge channels is one-dimensional [2] and scattering between different channels can be extremely small [4,5].

Another interesting result of studying ballistic transport is the discovery of the quantized conductance of short narrow wires or quantum point contacts (QPCs) at zero magnetic field. The conductance of QPCs is quantized at multiple values of $2e^2/h$, due to the formation of one-dimensional (1D) subbands in the constriction [6,7]. It was shown that in high magnetic fields QPCs can be used as selective transmitters of edge channels [8]. Edge channels with different Landau level index can either be transmitted or reflected by a QPC. This enables one to study transport occurring in a selected edge channel, by selective current population or voltage detection of a particular edge channel [8].

We have employed the properties of edge channels and QPCs for the construction of a 1D electron interferometer, in which discrete zero-dimensional (0D) states are observed [9]. The reduction to zero dimensions is obtained by confining a 1D edge channel in a quantum dot between two partially transparent barriers. The transparency of the barriers allows a coupling to the 0D states for electronic

0039-6028/90/$ 03.50

transport measurements. The 0D states show up as pronounced oscillations in the conductance with maxima occurring whenever the energy of a 0D state coincides with the Fermi energy. Electron transfer then takes place through resonant transmission. The experimental results are in good agreement with theory and confirm the Landauer–Büttiker description of confined electron transport in a quantizing magnetic field.

2. Device description

Fig. 1 shows the schematic layout of our device. A Hall-bar is defined in the 2DEG of a high mobility GaAs/AlGaAs heterostructure. The 2DEG has a transport mean free path of 9 μm and an electron density of 2.3×10^{15} m^{-2}. On top of the heterostructure two pairs A and B of metallic gates are fabricated by standard optical and electron beam lithographic techniques. A negative voltage of -0.2 V on both gate pairs depletes the electron gas underneath the gates and creates a quantum dot with a diameter of 1.5 μm in the 2DEG. The narrow channel separating the gate pairs is already pinched off at this gate voltage. To allow electronic transport, connection from the wide 2DEG regions to the dot is arranged by two 300 nm wide QPCs. The transport properties of each individual QPC can be studied by applying the gate voltage to only one gate pair and zero voltage to the other. The electrostatic potential landscape at the QPC resembles a saddled shaped barrier. The height of the barrier E_B can be increased by reducing the gate voltage until the QPC is pinched off at -1 V.

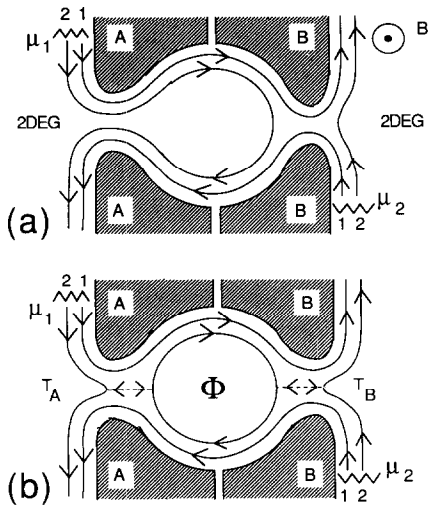

Fig. 1. Schematic layout of the quantum dot with diameter of 1.5 μm and two 300 nm wide quantum point contacts. The electron flow in edge channels is shown when a high magnetic field B is applied. (a) illustrates adiabatic transport for unequal QPCs A and B. (b) A 1D loop is formed when an edge channel is only partially transmitted by both QPCs.

3. Edge channels and selective transmission of QPCs

In this section we describe the main properties of edge channels and the selective transmission of them by QPCs. In a high magnetic field the energy of the electrons is given by

$$E_n=(n-\tfrac{1}{2})\hbar\omega_c\pm\tfrac{1}{2}g\mu_B B+eV(x,y)\,, \qquad (1)$$

with n the Landau level index, $g\mu_B B$ the spin splitting, and $V(x,y)$ the electrostatic potential, which will be nominally flat in the interior of the sample and rising at the boundary (see fig. 2). Electrostatic variations due to impurities are ignored because we are dealing with ballistic samples. The electron states at the left hand side of the sample are occupied to μ_1, the electrochemical potential of the current source, and their velocity direction is perpendicular to the cross-section of fig. 2. At the right hand side the electron states are filled up to μ_2, the electrochemical potential of the current drain and their velocity is in opposite direction. The difference in occupation $eV=\mu_1-\mu_2$ (determined by the voltage V between

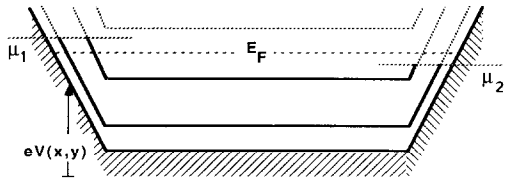

Fig. 2. Occupied electron states (bold) in Landau levels in the presence of a current flow, illustrating the formation of edge channels at the 2DEG boundary potential $V(x,y)$ where the Landau levels intersect the Fermi energy E_F.

current source and drain) between the two edges results in a net current flowing along the boundary of the sample. It can be shown [2] that the transport in edge channels is one-dimensional. From the well-known cancellation of density of states with velocity in one dimension it follows that the net current in each (spin split) Landau level is given by $I=(e/h)(\mu_1-\mu_2)$. The location of the current-carrying electron states elucidates the name of edge channels. The ratio current/voltage yields the quantized conductance e^2/h contributed by each occupied Landau level.

Although the above model is obviously highly simplified, it leads to some important features of transport in a high magnetic field. Büttiker [10] has pointed out that backscattering involves scattering between the opposite sample edges, which is suppressed when the current-carrying electrons with energies between μ_1 and μ_2 are not connected to the other boundary through available electron states. This is the case when the Fermi energy is between two bulk Landau levels (see fig. 2). Experimentally it was also shown that forward scattering between different edge channels at the same sample boundary is surprisingly low, even over macroscopic distances much larger than the zero field mean free path [4,5]. This means that the transport in edge channels is primarily adiabatic, i.e. with conservation of quantum index n. The fact that the transport in edge channels is adiabatic justifies they are being viewed as independent 1D current channels.

The relevant electron states for transport are only those at the Fermi energy E_F. The spatial location of the current-carrying electrons result from the condition $E_F=E_n$, yielding:

$$eV(x,y)=E_G=E_F-(n-\tfrac{1}{2})\hbar\omega_c\pm\tfrac{1}{2}g\mu_B B\,. \qquad (2)$$

E_G is known as the guiding energy [11]. Eq. (2) implies that edge channels with different Landau level index n or opposite spin direction, while all located at the sample boundary, follow different equipotential lines.

Using their controllable barrier height E_B, QPCs can be used as selective edge channel transmitters. Those edge channels for which $E_G<E_B$ will be reflected by a QPC and those with $E_G>E_B$ can pass through the QPC. Because only the transmitted edge channels contribute, the two-terminal conductance G of a single QPC is given by:

$$G=\frac{e^2}{h}(N+T)\,. \qquad (3)$$

Here N denotes the number of fully transmitted channels and T the partial transmission of the upper edge channel. From $E_B=E_B(V_g)$ and $E_G=E_G(B)$, it follows that the number of transmitted channels can be changed by varying the magnetic field or the gate voltage. Conductance quantization occurs in those intervals for B and V_g where $T=0$. From experiments [5,8] we know that eq. (3) holds very well, meaning that QPCs fully transmit the lower indexed edge channels (which follow higher equipotential lines, see eq. (2)) and partially transmit the upper channel without inducing scattering between the available (bulk) edge channels.

4. Adiabatic transport in series QPCs

When two QPCs are placed in series the question arises whether the series resistance in the ballistic transport regime is just the Ohmic addition of the individual QPC resistances [12]. We have studied this for the geometry of fig. 1, where the two QPCs are connected by a cavity. At zero magnetic field the incoming electrons will scatter randomly in the cavity and establish a more or less isotropic velocity distribution. In this way the cavity acts as a reservoir and the series resistance is just the Ohmic addition of the individual QPC resistances. This situation changes at a high magnetic field when the electron motion is confined to edge channels. If no scattering occurs between different channels the transport is adiabatic. The QPC with the highest barrier and consequently with the lowest number of transmitted channels will form the "bottleneck" for the total system. Those channels which can pass the highest barrier in the circuit can also pass the other barriers (see fig. 1a). The series conductance G_D then is completely determined by the smallest of the two conductances of the individual QPCs: $G_D=\min(G_A,G_B)$, where G_A and G_B are given by eq. (3).

If both QPCs transmit the same number of channels N and the upper edge channel is only partially

transmitted (see fig. 1b), the series conductance G_D is given by

$$G_D = \frac{e^2}{h}(N + T_D) . \quad (4)$$

The partial transmission T_D of the upper edge channel through the complete device can easily be calculated from the transmissions T_A and T_B of the individual QPCs. Ignoring interference effects which will be considered in the next section, an incoming electron will be directly transmitted through both QPCs with probability $T_A T_B$. After making one loop around the dot, the next probability to be transmitted is $T_A R_B R_A T_B$ (with $R = 1 - T$). A second loop gives $T_A (R_B R_A)^2 T_B$, etc. Summing all contributions yields for the total transmission probability

$$T_D = T_A T_B [1 + R_A R_B + (R_A R_B)^2 + \ldots]$$

$$= \frac{T_A T_B}{1 - R_A R_B} . \quad (5)$$

Eq. (5) is the classical result for the transmission of a single channel through two barriers.

In ref. [13] a detailed study is described on the transition from Ohmic transport (at $B = 0$ T) to adiabatic transport (at $B = 1$ T) in series QPCs. The measurements at $B = 1$ T and at a temperature of 0.6 K (so interference effects are averaged out) are shown in fig. 3. The conductances G_A and G_B measured with zero voltage applied to the other gate pair, show (spin degenerate) plateaus at integer multiples of $2e^2/h$. The series conductance G_D plotted in fig. 3a is measured with equal voltage applied to both gate pairs. G_D also shows quantized plateaus whenever both conductances G_A and G_B are quantized. The step height of $2e^2/h$ indicates adiabatic transport through the series QPC device. Scattering between different edge channels would yield smaller steps (which is observed for $B < 1$, see ref. [13]). The transition regions between the plateaus are in good agreement with a calculation from eq. (5) (not shown here). A further test if adiabatic transport takes place is shown in fig. 3b. In this experiment the gate voltage V_g on pair A is fixed at -0.7 V and the voltage on gate pair B is varied. The series conductance should now be equal to $G_A = 4e^2/h$ for $V_g > -0.7$ V and equal to G_B for $V_g < -0.7$ V. Comparing fig. 3b with fig. 3a it can be seen that the series conductance is indeed in good agreement with $G_D = \min(G_A, G_B)$. *We conclude that the transport through the series QPC device is adiabatic, whenever the transport through edge channels take place at a sufficiently high magnetic field.*

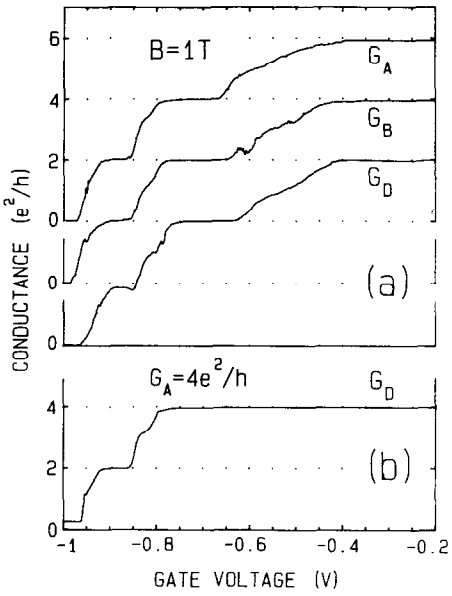

Fig. 3. Conductances G_A and G_B of the individual QPCs and G_D of the two QPCs in series illustrating adiabatic transport at $B = 1$ T. (a) For equal voltage on both gate pairs A and B. (b) For fixed -0.7 V on gate pair A and varying the gate voltage on pair B.

5. Transport through 0D states

5.1. Theory

In the previous section we derived the classical transmission probability T_D for a 1D double barrier structure. Here we give a simple quantum mechanical derivation for which the electron wave function must be taken as a starting point [14]. Consider an incoming wave Ψ_{in} from the left in the partial transmitted edge channel of fig. 1b. The right- and left-moving waves Ψ_R and Ψ_L in the dot are mutually connected through: $\Psi_R = \sqrt{T_A}\,\Psi_{in} + \sqrt{R_A}\,\Psi_L$ and $\Psi_L = \sqrt{R_B}\,\Psi_R \exp(i\upsilon)$, when both are evaluated at

QPC A. υ denotes the acquired phase after making one revolution around the dot. With $\Psi_{out} = \sqrt{T_B}\Psi_R$ for the outcoming wave at the right, the transmission probability $T_D = |\Psi_{out}|^2/|\Psi_{in}|^2$ is given by:

$$T_D = \frac{T_A T_B}{1 - 2\sqrt{R_A R_B}\cos\upsilon + R_A R_B}. \quad (6)$$

Eq. (6) implies that the transmission T_D and thus the conductance G_D oscillate as a function of the phase factor υ, whenever both barrier transmissions T_A and T_B differ from zero. υ is determined by the enclosed flux: $\upsilon = 2\pi BA/\phi_0$, where A denotes the area enclosed by the edge channel loop and $\phi_0 = h/e$ is the flux quantum. Whenever the enclosed flux $\Phi = BA$ equals an integer number of flux quanta the transmission T_D is resonant. The amplitude of the oscillations is determined by the barrier transmissions T_A and T_B. It follows from eq. (6) that for $T_A = T_B$ the transmission at resonance gives $T_D = 1$ and the conductance G_D then equals e^2/h. For asymmetric transmissions $T_A \neq T_B$ the maximum value of T_D is less than 1. The minimum value of T_D between two resonant states approaches zero for small barrier transmissions. Note that eq. (6) is exactly the formula for a 1D interferometer. While in our case the phase is determined by the enclosed flux, eq. (6) also holds for a cavity inbetween two barriers, where the product of cavity length and longitudinal wave vector determines the phase υ.

The resonance results from the formation of 0D states in the confined edge channel due to the small circumference of this 1D loop. Resonant transmission occurs whenever the Fermi energy E_F coincides with a 0D state. This becomes more clear for very weak coupling ($T_A = T_B \approx 0$) to the quantum dot. Then the eigenstates of the dot are nearly undisturbed and eq. (6) gives sharp Lorentzian-shaped peaks belonging to discrete 0D-states. For $T_A = T_B \approx 0$ the peak amplitude approaches 100% of e^2/h.

The above considerations are general for transport through 0D states. Similar properties were deduced from numerical calculations on the transmission of small quantum boxes in which 0D states are formed at zero magnetic field [15]. Also, recent transport experiments have shown the formation of 0D states due to electrostatic confinement in all three spatial dimensions [16].

5.2. Experiment

The two-terminal conductance measurements presented in this section are all performed at 6 mK. The conductance G_D of the quantum dot shows quantized plateaus as a function of magnetic field with a fixed gate voltage on both gate pairs. The plateaus ($T_D = 0$) indicate 1D transport through the dot, while at the transitions between the plateaus (when $T_D \neq 0$) transport through 0D states is expected.

Fig. 4 shows the transition from the second to the third plateau, which corresponds with the complete transmission of the lowest two edge channels and the partial transmission of the third. In figs. 4a and 4b the conductances G_A and G_B of the single QPCs are plotted, measured with -0.35 V on the corresponding gate pair. The increasing magnetic field gradually reduces the transmissions T_A and T_B of the third edge channel from 1 to 0. The irregular structure can be

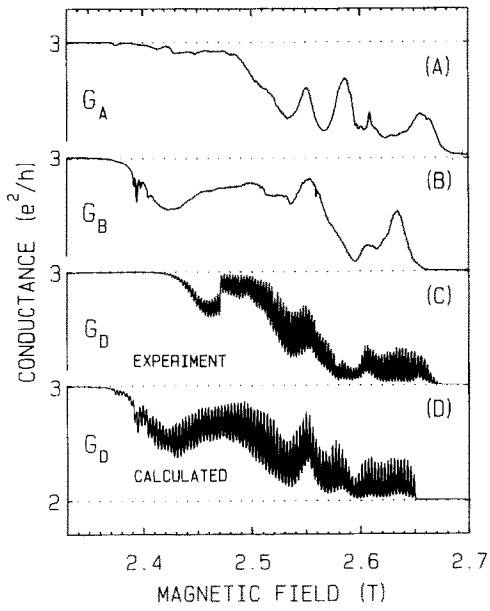

Fig. 4. Transition from the second to the third plateau of the QPC conductances G_A (a) and G_B (b) and of the dot G_D (c). Large oscillations are seen in G_D whenever both G_A and G_B are not quantized. A calculation of G_D from eq. (6) with the measured G_A and G_B is shown in (d); see text.

attributed to random interferences within the QPCs themselves [17]. The conductance G_D of the dot is shown in fig. 4c, which is measured with $V_g = -0.35$ V on both gate pairs. Large oscillations are seen in-between the plateau regions. The amplitude modulation of the oscillations is up to 40% of e^2/h. The fact that the oscillations do not exceed $3e^2/h$ nor drop below $2e^2/h$ indicates that the oscillations originate from the third edge channel only. The curve plotted in fig. 4d is calculated from eq. (6) with the measured conductances G_A and G_B. We will discuss the comparison between theory and experiment in more detail below.

Fig. 5a shows the oscillations on an expanded scale, and illustrates their regularity. The period B_o of the oscillations smoothly varies from $B_o = 2.5$ mT at $B = 2.5$ T to $B_o = 2.8$ mT at $B = 2.7$ T. In fig. 5b the region of low transmission is shown. Here the conductance contribution of the third edge channel is nearly zero except when the Fermi energy coincides with the energy of a 0D state. *The discrete peaks clearly demonstrate the resonant transmission through the quantum dot.*

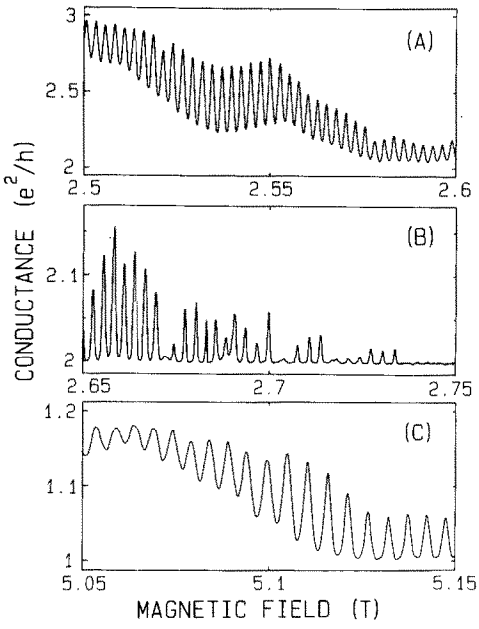

Fig. 5. (a) Enlarged oscillations from fig. 4c showing their regularity (period $B_o = 2.5$ mT). (b) Region of low transmissions of the third edge channel ($G_A, G_B \approx 2$). The discrete conductance peaks demonstrate resonant transmission through 0D states. (c) Oscillatons belonging to the second edge channel (period $B_o = 5.3$ mT).

0D states belonging to other partially transmitted edge channels are also observed. In fig. 5c the oscillations are shown which originate from the second channel. A striking feature is that the period ($B_o = 5.3$ mT at $B = 5.1$ T) differs from the period of the oscillations belonging to the third edge channel. Also the observed oscillations from the fourth ($B_o = 2.1$ mT at $B = 1.85$ T) and fifth ($B_o = 1.4$ mT at $B = 1.25$ T) edge channels differ in their period. The origin of the difference in period for different edge channels will be discussed below. *The observation of a distinct period for each transition again indicates that the oscillations originate from a single edge channel only.*

To estimate the energy separation between consecutive 0D states, we have measured the oscillations for different temperatures and voltages across the sample. The oscillations disappear above 200 mK and 40 μV, which both lead to an energy separation of about 40 μeV.

A second way to change the flux is by changing the area enclosed by the confined edge channel. This is accomplished by varying the gate voltage at a fixed magnetic field. Fig. 6a shows the 0D states for $B = 2.5$ T and a changing gate voltage on both gate pairs. The oscillation period is 1 mV. For a fixed voltage (-0.35 V) on one gate pair and a changing voltage on the

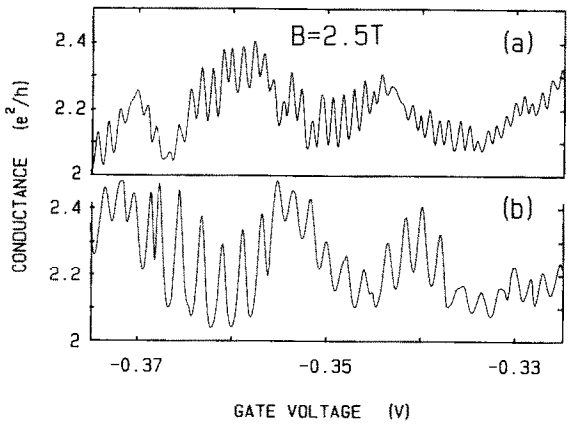

Fig. 6. Conductance oscillations as a function of gate voltage for a fixed magnetic field $B = 2.5$ T. In (a) the voltage on both gate pairs is varied (period = 1 mV) and in (b) the gate voltage on one pair is kep fixed at -0.35 V and varied on the other gate pair (period = 2 mV).

other pair the observed period is 2 mV, as can be seen in fig. 6b. Assuming that in the latter case only half of the area in the dot is effected, we conclude that a variation in gate voltage changes the area enclosed by the edge channels. *Thus our device also provides an electrostatic control of the resonant transmission through 0D states.*

5.3. Discussion

In part 1 of this section we have discussed the fact that the amplitude modulation of the oscillations is determined by the barrier transmissions T_A and T_B. To compare the measured modulation with eq. (6) we can use the conductances G_A and G_B of the individual QPCs (figs. 4a and 4b) in the expression for T_D. The calculated conductance G_D is shown in fig. 4d. We have included temperature averaging in the calculation with the expression $G_D = \int G_D(E)\,[\partial f/\partial E]\,dE$ in which $f(E,T)$ is the Fermi distribution function and $G_D(E)$ the energy dependent conductance at zero temperature. The latter can be obtained from eqs. (4) and (6) by noting that a change in phase of 2π corresponds to a change in energy of 40 μeV. Note that by averaging of eq. (6) over a large energy range (larger than the energy range corresponding to a change in phase of 2π) the classical result of eq. (5) is obtained. We have chosen a fixed period of 3 mT in the calculation and an effective temperature of 20 mK, which is the sample temperature (6 mK) plus a contribution from the voltage (≈ 6 μV) across the sample. Comparing the measured (fig. 4c) and the calculated (fig. 4d) conductance G_D, it can be seen that these are in good agreement. Also the shape of the oscillations which is rounded for strong coupling and peaked for weak coupling, appears the same in the measurements as in the calculation. The exact modulation is not reproduced in the calculation, which is probably due to a slight mutual influence between the gate pairs when both are turned on.

The conductance oscillations described in this paper are reminiscent of the Aharonov–Bohm effect observed in small metal [18] and semiconductor rings [19]. However, in these systems the electrons are already confined in a ring in the absence of a magnetic field. The conductance of such rings oscillates as a function B with a period ϕ_o/A (A is the fixed area enclosed by the ring) even if the wires are not 1D. In fact this Aharonov–Bohm effect quenches for high magnetic fields when edge channels are formed in the wires [19]. In contrast to this, edge channels are the starting point for the occurrence of oscillations in the quantum dot. The period of our oscillations is also not simply determined by the dot area because of the change in location of the edge channels when the magnetic field is varied. The change in radius Δr of the edge channel loop follows from eq. (2) as: $\Delta r = \Delta V(x,y)/E = \Delta E_G/(eE)$ which varies with the magnetic field, differs for different indices n or spin direction, and depends on the "hardness" of the boundary potential given by the radial electric field E. Assuming circular symmetry for the edge channel loop we can write the change in enclosed flux $\Delta\Phi$ resulting from a change in field ΔB as:

$$\Delta\Phi = \Delta(B\pi r^2) = \pi r^2 \Delta B + B 2\pi r \Delta r$$
$$= \left(\pi r^2 + \frac{B 2\pi r}{eE}\frac{\partial E_G}{\partial B}\right)\Delta B\,. \qquad (7)$$

Evaluation of eq. (7) with $r = 750$ nm, $B = 2.5$ T and a rough estimate $E \approx 10^4$–15^5 V/m shows that the second term (which is negative!) can be of the same order of magnitude as the first term [#1] The observed period $B_o = \phi_o \Delta B/\Delta\Phi$ is therefore not simply determined by the enclosed area. The observation of distinct periods at different transitions, well separated by quantized regions, shows that the oscillations orginate from single 1D edge channels. This conclusion provides strong evidence that *in the ballistic quantum Hall regime the net current is completely carried by edge channels.*

6. Concluding remarks

Edge channels in combination with QPCs provide a simple and elegant system for studying electron transport of reduced dimensionality. Using the adjustable barriers of QPCs we have realized a 1D elec-

[#1] At the 2DEG boundary the electrostatic potential changes by an amount E_F/e (≈ 9 mV) in a depletion region which is about 300 nm wide. This gives a typical field strength $E \approx 3 \times 10^4$ V/m. A derivation of the period is also given by L.I. Glazman and M. Jonson in ref. [13].

tron interferometer. The rigidity of edge channels is illustrated by the occurrence of adiabatic transport through the series QPC device. Single electron states are formed when a 1D edge channel is confined between two barriers. These 0D states can be tuned by varying the magnetic field and the gate voltage. The resonant transmission through 0D states is clearly observed as regular oscillations in the conductance. The experiment confirmes the edge channel description of transport in the ballistic quantum Hall regime.

Acknowledgements

We thank L.W. Molenkamp and A.A.M. Staring for valuable discussions, W. Kool for assistance with the experiments, M.E.I. Broekaart, S. Phelps and C.E. Timmering at the Philips Mask Centre, C.T. Foxon, J.J. Harris and the Delft Centre for Submicron Technology for their contribution in the fabrication of the devices, and the Stichting FOM for financial support.

References

[1] G. Timp, A.M. Chang, P. Mankiewich, R. Behringer, J.E. Cunningham, T.Y. Chang and R.E. Howard, Phys. Rev. Lett. 59 (1987) 732;
M.L. Roukes, A. Scherer, S.J. Allen, H.G. Craighead, R.M. Ruthen, E.D. Beebe and J.P. Harbison, Phys. Rev. Lett. 59 (1987) 3011;
B.E. Kane, D.C. Tsui and G. Weimann, Phys. Rev. Lett. 59 (1987) 1353.

[2] B.I. Halperin, Phys. Rev. B 25 (1982) 2185.

[3] P. Streda, J. Kucera and A.H. MacDonald, Phys. Rev. Lett. 59 (1987) 1973;
J.K. Jain and S.A. Kivelson, Phys. Rev. Lett. 60 (1988) 1542.

[4] S. Komiyama, H.Hirai, S. Sasa and S. Hiyamizu, preprint.

[5] B.J. van Wees, E.M.M. Willems, L.P. Kouwenhoven, C.J.P.M. Harmans, J.G. Williamson, C.T. Foxon and J.J. Harris, Phys Rev. B 39 (1989) 8066.

[6] D.A. Wharam, T.J. Thornton, R. Newbury, M. Pepper, H. Ahmed, J.E.F. Frost, D.G. Hasko, D.C. Peacock, D.A. Ritchie and G.A.C. Jones, J. Phys. C 21 (1988) L209.

[7] B.J. van Wees, H. van Houten, C.W.J. Beenakker, J.G. Williamson, L.P. Kouwenhoven, D. van der Marel and C.T. Foxon, Phys. Rev. Lett. 60 (1988) 848.

[8] B.J. van Wees, E.M.M. Willems, C.J.P.M. Harmans, C.W.J. Beenakker, H. van Houten, J.G. Williamson, C.T. Foxon and J.J. Harris, Phys. Rev. Lett. 62 (1989) 1181.

[9] The main results of this paper are also described in: B.J. van Wees, L.P. Kouwenhoven, C.J.P.M. Harmans, J.G. Williamson, C.E. Timmering, M.E.I. Broekaart, C.T. Foxon and J.J. Harris, Phys. Rev. Lett. 62 (1989) 2523;
L.P. Kouwenhoven, B.J. van Wees, C.J.P.M. Harmans and J.G. Williamson, Proc. of the Workshop on Science and Engineering of 1- and 0-dimensional Semiconductors, Eds. C.M. Sotomayor-Torres and S.P. Beaumont (Plenum, New York), to be published.

[10] M. Büttiker, Phys. Rev. B 38 (1988) 9375.

[11] The Quantum Hall Effect, Eds. R.E.Prange and S.M. Girvin (Springer, New York, 1987).

[12] This has been studied first by: D.A. Wharam, M. Pepper, A. Ahmed, J.E.F. Frost, D.G. Hasko, D.C. Peacock, D.A. Ritchie and G.A.C. Jones, J. Phys. C 21 (1988) L887;
A theoretical study is described in: C.W.J. Beenakker and H. van Houten, Phys. Rev. B 39 (1989) 10445.

[13] L.P. Kouwenhoven, B.J. van Wees, W. Kool, C.J.P.M. Harmans, A.A.M. Staring and C.T. Foxon, Phys. Rev. B 40 (1989) 8083.
General conditions for the occurrence of adiabatic transport are described by: L.I. Glazman and M. Jonson, J. Phys. Condens. Matter 1 (1989) 5547.

[14] A theoretical study of a 2D dot to which narrow leads are attached is given by U. Sivan, Y. Imry and C. Hartzstein, Phys. Rev. B 39 (1989) 1242;
U. Sivan and Y. Imry, Phys. Rev. Lett. 61 (1988) 1001.

[15] D. van der Marel, Proc. Symp. on Nanostructure Physics and Fabrication, Eds. W.P. Kirk and M. Reed (Academic Press, New York, 1989).

[16] M.A. Reeds, J.N. Randall, R.J. Aggarwal, R.J. Matyi, T.M. Moore and A.E. Wetsel, Phys. Rev. Lett. 60 (1988) 535;
T.P. Smith III, K.Y Lee, C.M. Knoedler, J.M. Hong and D.P. Kern, Phys. Rev. B 38 (1988) 2172;
C.G. Smith, M. Pepper, H. Admed, J.E.F. Frost, D.G. Hasko, D.C. Peacock, D.A. Ritchie, and G.A.C. Jones, J. Phys. C. (Solid State Phys.) 21 (1988) L893.

[17] Regular Aharonov-Bohm oscillations in a single QPC have been reported by: P.H.M. van Loosdrecht, C.W.J. Beenakker, H. van Houten, J.G. Williamson, B.J. van Wees, J.E. Mooij, C.T. Foxon and J.J. Harris, Phys. Rev. B 38 (1988) 10162.

[18] R.A. Webb, S. Washburn, C.P. Umbach and R.B. Laibowitz, Phys. Rev. Lett. 54 (1985) 2696.

[19] G. Timp, A.M. Chang, J.E. Cunningham, T.Y. Chang, P. Mankiewich, R. Behringer and R.E. Howard, Phys. Rev. Lett. 58 (1987) 2814;
C.J.B. Ford, T.J. Thornton, R. Newbury, M. Pepper, H. Ahmed, C.T. Foxon, J.J. Harris and C. Roberts, J. Phys. C. (Solid State Phys.) 21 (1988) L325;
G. Timp, P.M. Mankiewich, P. de Vegvar, R. Behringer, J.E. Cunningham, R.E. Howard, H.U. Baranger and J.K. Jain, Phys. Rev. B 39 (1989) 6227.